

paramount for *B. fragilis* to maintain a long-term commensal relationship in the human colon. As *B. fragilis* is the anaerobic species most frequently isolated from clinical infections, and the capsular polysaccharides are instrumental in the disease process, phase variation may also contribute to the pathogenic potential of this organism. □

Methods

Construction of insertion mutants

Sequences of primers used in this study are listed in Supplementary Information Table 2. DNA used for homologous recombination for each of the four mutants was amplified by PCR from NCTC9343 using the following primers: PSE: U1-F, UpE-R; PSF: U2-F, UpF-R; PSG: UY5-F, UpG-R; PSH: Y6F2, UpH-R. These 2.1–3.3-kb products were digested with *Bam*HI and cloned into pJST55 (ref. 9). Plasmids were introduced into *B. fragilis* NCTC9343 by mobilization from *E. coli* and cointegrates were selected using erythromycin.

Demonstration of inversion and PCR/digestion technique

Primers used to demonstrate inversion—in the order of upstream primer, primer between the inverted repeats and downstream primer—are as follows: PSE: UpE-1, UpE-2, UpE-3; PSF: UpF-1, UpF-2, UpF-3; PSG: UpG-1, UpG-2, UpG-3; PSH: UpH-1, UpH-2, UpH-3.

For the PCR/digestion technique in Fig. 4b, c, a PCR is performed, using chromosomal DNA from a phenotypically selected population, which amplifies the PSA or PSB invertible region and some flanking DNA. The PCR product is digested with a restriction enzyme that cleaves asymmetrically between the inverted repeat elements. When the promoter is in one orientation, the two fragments resulting from the digested PCR product differ in size from those fragments that result when the promoter is in the opposite orientation.

PSF and PSG inversion junctions

Inversion junctions were determined by sequencing PCR products resulting from amplification using the following primers that only amplify DNA in one orientation: PSF: UpF-2, UpF-3; PSG: UpG-2, UpG-3.

Creation of *xylE* reporter constructs

The 420-bp region upstream of *upaY* was amplified by PCR using primers PMA-1 and PMA-3, and was cloned into the *Bam*HI site of *xylE* reporter plasmid pLEC23. The following primer pairs were used for PCR amplification of the invertible regions lacking 7–9 bp of each inverted repeat: PSA: IRA-F, IRA-R; PSB: IRB-F, IRB-R; PSD: IRD-F, IRD-R; PSE: IRE-F, IRE-R; PSF: IRF-F, IRF-R; PSG: IRG-F, IRG-R; PSH: IRH-F, IRH-R. Each PCR product was cloned into pLEC23 in both orientations. XylE assay was performed as described (C.M.K., D. Lipsett and L.E.C., unpublished work).

Received 6 August; accepted 3 October 2001.

1. Macpherson, A. et al. A primitive T cell-independent mechanism of intestinal mucosal IgA responses to commensal bacteria. *Science* **288**, 2222–2226 (2000).
2. Comstock, L. E. et al. Analysis of a capsular polysaccharide biosynthesis locus of *Bacteroides fragilis*. *Infect. Immun.* **67**, 3525–3532 (1999).
3. Coyne, M. J., Kalka-Moll, W., Tzianabos, A. O., Kasper, D. L. & Comstock, L. E. *Bacteroides fragilis* NCTC9343 produces at least three distinct capsular polysaccharides: cloning, characterization, and reassignment of the PS B and PS C biosynthesis loci. *Infect. Immun.* **68**, 6176–6181 (2000).
4. Coyne, M., Tzianabos, A., Mallory, B., Kasper, D. & Comstock, L. A polysaccharide biosynthesis locus required for virulence of *Bacteroides fragilis*. *Infect Immun* **69**, 4342–4350 (2001).
5. Bayley, D., Rocha, E. & Smith, C. Analysis of *cepA* and other *Bacteroides fragilis* genes reveals a unique promoter structure. *FEMS Microbiol. Lett.* **193**, 149–154 (2000).
6. Kim, J. et al. *In vivo* phase variation of *Escherichia coli* type 1 fimbrial genes in women with urinary tract infection. *Infect. Immun.* **66**, 3303–3310 (1998).
7. Abraham, J., Freitag, C., Clements, J. & Eisenstein, B. An invertible element of DNA controls phase variation of type 1 fimbriae of *Escherichia coli*. *Proc. Natl Acad. Sci. USA* **82**, 5724–5727 (1985).
8. Olsen, P. & Klemm, P. Localization of promoters in the *fim* gene cluster and the effect of H-NS on the transcription of *fimB* and *fimE*. *FEMS Microbiol. Lett.* **116**, 95–100 (1994).
9. Thompson, J. S. & Malamy, M. H. Sequencing the gene for an imipenem-cefoxitin-hydrolyzing enzyme (CfA) from *Bacteroides fragilis*. *J. Bacteriol.* **172**, 2584–2593 (1990).

Supplementary Information accompanies the paper on Nature's website (<http://www.nature.com>).

Acknowledgements

We thank W. Kalka-Moll for electron microscope photography and J. Daley and S. Lazo-Kallanian for assistance with FACS analysis. This work was supported by grants from the National Institutes of Health.

Competing interests statement

The authors declare that they have no competing financial interests.

Correspondence and requests for materials should be addressed to L.E.C. (e-mail: lcomstock@channing.harvard.edu).

Barttin is a Cl⁻ channel β-subunit crucial for renal Cl⁻ reabsorption and inner ear K⁺ secretion

Raúl Estévez*, Thomas Boettger*, Valentin Stein*, Ralf Birkenhäger†, Edgar Otto†, Friedhelm Hildebrandt† & Thomas J. Jentsch*

* Zentrum für Molekulare Neurobiologie (ZMNH), Universität Hamburg, Falkenried 94, D-20246 Hamburg, Germany

† Universitäts-Kinderklinik, Universität Freiburg, Mathildenstrasse 1, D-79106 Freiburg, Germany

Renal salt loss in Bartter's syndrome is caused by impaired transepithelial transport in the loop of Henle. Sodium chloride is taken up apically by the combined activity of NKCC2 (Na⁺-K⁺-2Cl⁻ cotransporters) and ROMK potassium channels. Chloride ions exit from the cell through basolateral ClC-Kb chloride channels. Mutations in the three corresponding genes have been identified^{1–3} that correspond to Bartter's syndrome types 1–3. The gene⁴ encoding the integral membrane protein barttin is mutated in a form of Bartter's syndrome that is associated with congenital

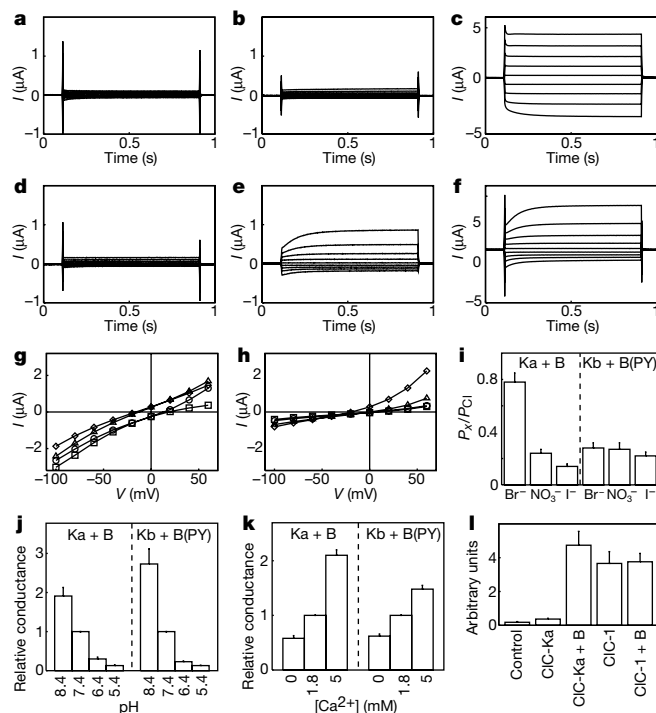


Figure 1 Functional characterization of ClC-K/barttin in *Xenopus* oocytes. **a–f**, Measurements of current (*I*). Barttin (**a**), ClC-Ka (**b**) and ClC-Kb (**d**) alone gave no significant currents. ClC-Ka/barttin co-expression gave large currents (**c**), and ClC-Kb/barttin moderate currents (**e**). **f**, ClC-Kb/barttin(Y98A) currents. **g, h**, Steady-state current–voltage relationships for ClC-Ka/barttin and ClC-Kb/barttin(Y98A), respectively, in the presence of: Cl⁻, diamonds; Br⁻, triangles; NO₃⁻, circles; I⁻, squares. **i**, Permeability ratios (*P_X/P_{Cl}*) from reversal potentials for ClC-Ka/barttin (left) and ClC-Kb/barttin(Y98A) (right). Averages from at least two batches of oocytes, five oocytes per batch. **j**, Effect of extracellular pH on ClC-Ka/barttin (left) and ClC-Kb/barttin(Y98A). **k**, Effect of extracellular Ca²⁺ on ClC-Ka/barttin (left) and ClC-Kb/barttin(Y98A). In **j** and **k**, conductances at –20 mV were normalized to values at pH 7.4 or 1.8 mM Ca²⁺, respectively (two or three batches of oocytes, 5–9 oocytes per batch). **l**, Surface expression¹³ of epitope-tagged ClC-Ka. ClC-Ka with a cytoplasmic HA tag (left) and extracellularly tagged ClC-1 served as controls. B, barttin; B(PY), barttin(Y98A). Averages from 7–13 oocytes. Voltage (*V*) was clamped between +80 and –100 mV for 0.8 s in 20-mV steps throughout. Error bars, s.e.m.

deafness and renal failure. Here we show that barttin acts as an essential β -subunit for ClC-Ka and ClC-Kb chloride channels, with which it colocalizes in basolateral membranes of renal tubules and of potassium-secreting epithelia of the inner ear. Disease-causing mutations in either ClC-Kb or barttin compromise currents through heteromeric channels. Currents can be stimulated further by mutating a proline-tyrosine (PY) motif on barttin. This work describes the first known β -subunit for ClC chloride channels and reveals that heteromers formed by ClC-K and barttin are crucial for renal salt reabsorption and potassium recycling in the inner ear⁵.

ClC-Ka and ClC-Kb are highly homologous Cl⁻ channels that are nearly exclusively expressed in kidney⁶. *CLCNKB* mutations in Bartter's syndrome³ together with immunohistochemical results^{7,8} suggest that human ClC-Kb (the orthologue of rodent ClC-K2) mediates basolateral Cl⁻ efflux in the thick ascending limb of Henle's loop and in more distal nephron segments. Similarly, immunolocalization⁹ and the diabetes insipidus observed in *Clnk1*^{-/-} mice¹⁰ indicate that rodent ClC-K1 (the orthologue of human ClC-Ka) is crucial for transepithelial transport in the thin ascending limb. Whereas ClC-K1 yields Cl⁻ currents on heterologous expression^{11,12}, no currents are observed with human ClC-Ka or ClC-Kb^{6,12}, suggesting that ClC-K channels may need β -subunits.

Positional cloning of the gene *BSND*, which underlies Bartter's syndrome type 4 (also named BSND; OMIM accession number 602522), identified barttin⁴. When barttin was co-expressed with ClC-Ka in *Xenopus* oocytes, large Cl⁻ currents were observed (Fig. 1c). No currents were seen with barttin, ClC-Ka or ClC-Kb alone (Fig. 1a, b, d). In oocytes, barttin/ClC-Kb co-expression gave small but detectable currents (Fig. 1e). More pronounced effects on ClC-Kb were seen in transfected tsA201 cells (see Supplementary Information A), and in oocytes injected with an activating mutant of barttin (Y98A; see below) (Fig. 1f). In oocytes, voltage activation differed between ClC-Ka/barttin and ClC-Kb/barttin (Fig. 1c, e, f). No such difference was found in mammalian cells (see Supplementary Information A). Barttin also markedly increased currents of rat ClC-K1, which yields small currents by itself^{11,12} (Fig. 2b). The effect seemed to be specific for ClC-K because currents of ClC-1, ClC-2 and ClC-5 were not changed by barttin (data not shown). Barttin

enhanced the surface expression^{13,14} of ClC-Ka, but not of the muscle channel ClC-1 (Fig. 1l).

Ion substitution revealed that both ClC-Ka/barttin and ClC-Kb/barttin were anion selective (Fig. 1g–i). As is typical for the ClC family¹⁵, they conducted Cl⁻ better than Γ . Permeability sequences were Cl⁻ \geq Br⁻ > NO₃⁻ > Γ for ClC-Ka/barttin, and Cl⁻ > Br⁻ = NO₃⁻ \geq Γ for ClC-Kb/barttin (Fig. 1i). Heteromeric ClC-K/barttin channels were sensitive to extracellular pH (Fig. 1j) and Ca²⁺ (Fig. 1k). The inhibition of ClC-Ka/barttin by low extracellular pH and its stimulation by extracellular Ca²⁺ compares well to rat ClC-K1 expressed by itself^{9,12}. Compared with ClC-Ka/barttin, ClC-Kb/barttin is more sensitive to pH and less responsive to Ca²⁺.

Barttin has two hydrophobic stretches that may span the membrane (ref. 4; Fig. 2a). Epitope-tagging experiments supported this model by indicating that the first hydrophobic stretch is not a cleavable signal peptide (see Supplementary Information B). Consistent with the poor conservation between species of the second half of barttin⁴, and with the observation that all described disease-causing mutations affect the amino-terminal half⁴, large portions of the carboxy terminus could be deleted without abolishing the stimulatory effect on ClC-K1 (Fig. 2b). Truncating the protein before residue 85, however, destroyed function. The deleted segment contains a putative PY motif^{16,17} (Fig. 2a). When the critical tyrosine residue¹⁷ was mutated (Y98A), stimulation of ClC-Ka and ClC-Kb currents by barttin was enhanced (Figs 1f and 2c). Macroscopic currents did not differ qualitatively from those of wild-type heteromers. Because ClC-Kb/barttin currents are small in oocytes, this activating mutant was used to reliably investigate properties of heteromeric ClC-Kb (Fig. 1f, h–k). The effects of this mutation resemble results obtained with the Na⁺ channel ENaC^{16,17} and the Cl⁻ channel ClC-5 (ref. 14). In those cases, the increase in currents depended on an interaction of their PY motifs with WW domains of ubiquitin protein ligases^{14,18}. Future work will reveal whether WW-domain proteins are physiological regulators of ClC-K/barttin channels.

In addition to deletions and truncations, missense mutations in the N-terminal part of barttin (Fig. 2a) are associated with BSND⁴. Most of these mutations abolished or decreased the stimulatory effect on ClC-Ka or ClC-Kb (Fig. 3a, b). In the two cases that were investigated (R8L and R8W), the mutated proteins failed to increase surface expression of ClC-Ka (data not shown). Surprisingly, one missense mutation (G10S) increased ClC-Ka currents over those obtained with wild-type barttin, and did not reduce effects on ClC-Kb when studied in the framework of the activating Y98A mutant (Fig. 3a, b). Hence this mutation might cause disease by a mechanism that is not reflected in our expression system. Disease-causing missense mutations of ClC-Kb^{3,19} resulted in significant reductions or the loss of ClC-Kb/barttin currents (Fig. 3c).

In situ hybridization showed barttin expression in specific nephron segments and in the stria vascularis⁴. If barttin acts as a β -subunit for ClC-Ka and ClC-Kb, these proteins should colocalize in membranes. Immunofluorescence revealed that all nephron

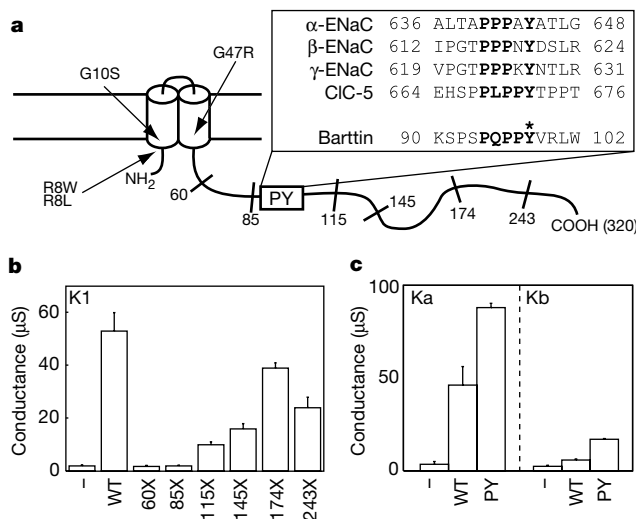


Figure 2 Basic structural and functional features of barttin. **a**, Proposed topology. Described⁴ and newly identified (G47R; data not shown) mutations are indicated. The PY motif^{16,17} (box) is compared with similar motifs of ENaC^{16,17} and ClC-5 (ref. 14) (inset). The asterisk shows the tyrosine mutated to alanine in barttin (Y98A). Truncations are indicated by slashes and the number of the stop codon. **b**, Effect of truncated barttin on ClC-K1 in oocytes. Averaged conductances at -20 mV of two batches (11 oocytes). **c**, Effect of the PY-motif mutation Y98A ('PY') on ClC-Ka (left) and ClC-Kb (right). Normalized currents of 15 oocytes from three batches. WT, wild type.

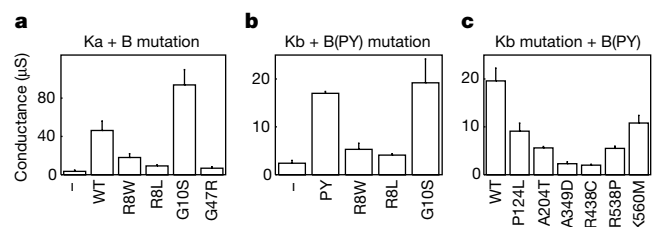


Figure 3 Functional consequences of disease-associated mutations in *Xenopus* oocytes. **a**, **b**, Effect of barttin (B) missense mutations⁴ on ClC-Ka (**a**) and ClC-Kb (**b**). **c**, Effects of *CLCNKB* missense mutations^{3,19} on ClC-Kb/barttin. In **b** and **c**, barttin (Y98A) was used to obtain sufficient currents. Conductances at -20 mV are averages of 7–25 oocytes each. WT, wild type.

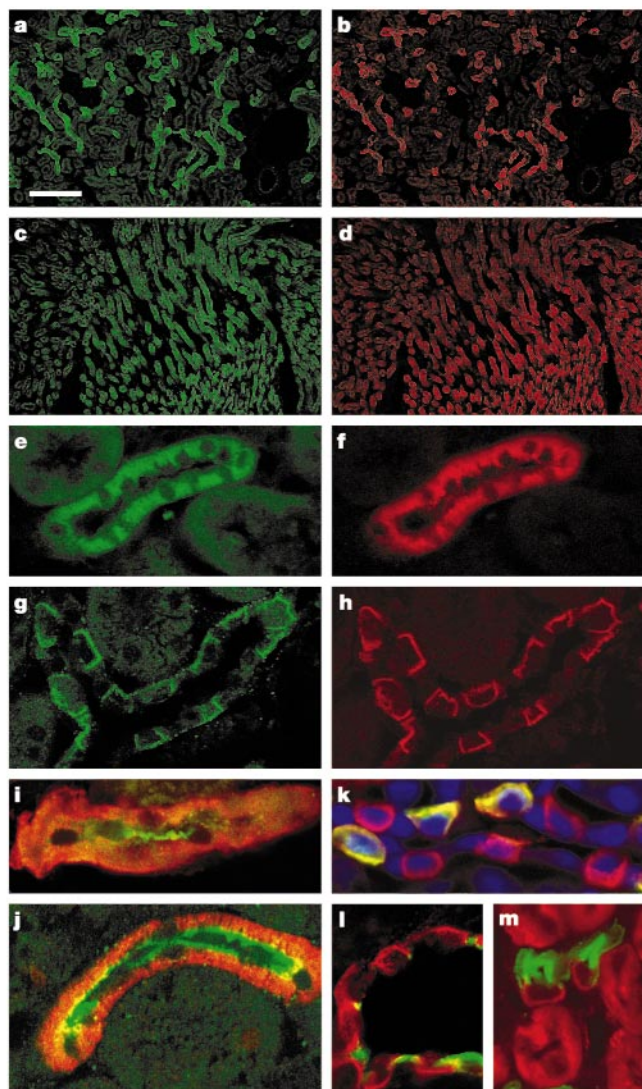


Figure 4 Barttin and CIC-K proteins in murine kidney. **a–d**, Overviews of renal cortex (**a, b**) and medulla (**c, d**) reveal strict co-expression of CIC-K (**a, c**) and barttin (**b, d**). **e, f**, Thick ascending limb (TAL) stained for CIC-K (**e**) and barttin (**f**). **g, h**, Intercalated cells of the cortical collecting duct (CCD) stained for CIC-K (**g**) and barttin (**h**). **i**, Tamm-Horsfall protein (green) identifies TAL segments that also express barttin (red). **j**, TAL showing ROMK K^+ channel (green) and barttin (red). **k**, Staining CCD for the anion exchanger AE1 (green) identifies α -intercalated cells²⁰. Barttin co-expression (red) yields a yellow stain. Cells expressing barttin and lacking AE1 are β -intercalated cells. Blue TOTO staining reveals nuclei. **l**, Aquaporin-2 (green) identifies²¹ CCD principal cells; intervening 'intercalated' cells express barttin (red). **m**, Medullary collecting ducts identified by aquaporin-2 staining (green); these and thin limbs of Henle's loop express barttin (red). Scale bar in **a** indicates 156 μm in **a–d**, 13 μm in **e–h** and **m**, and 10 μm in **i–l**.

segments expressing barttin also expressed CIC-K proteins and vice versa (Fig. 4a–h). As the CIC-K antibody⁷ does not distinguish between the highly homologous CIC-K1 and CIC-K2 proteins, this suggests that barttin forms heteromers with CIC-K1 (CIC-Ka) in the thin ascending limb of Henle⁹ (Fig. 4c, d, m), and with CIC-K2 (CIC-Kb) in the thick ascending limb and more distal segments⁸ (Fig. 4e–l). Staining for barttin and CIC-K was basolateral. The Tamm-Horsfall protein (Fig. 4i) and ROMK K^+ channels (Fig. 4j) are expressed in apical membranes of the thick ascending limb, the basolateral membranes of which stained for barttin (Fig. 4f, i, j) and CIC-K (Fig. 4e). Barttin was also detected in basolateral membranes of intercalated cells of the collecting duct (Fig. 4h, k, l), which are known to express CIC-K2 (CIC-Kb) as well⁸ (Fig. 4g). On the basis of the (green) staining for the basolateral anion exchanger AE1,

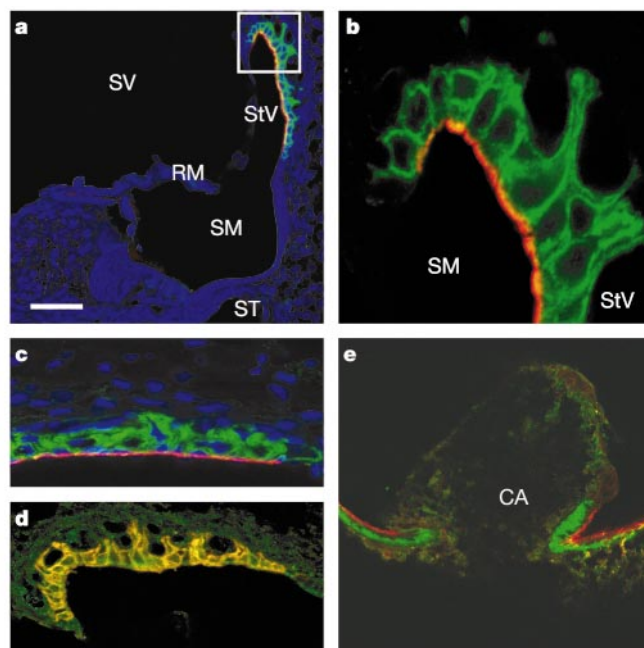


Figure 5 Barttin and CIC-K protein in the inner ear. **a**, Overview of a PO (postnatal day 0) mouse cochlea stained for barttin (green), KCNQ1 (red) and nuclei (blue). RM, Reissner's membrane (ruptured during sectioning); SM, scala media; ST, scala tympani; StV, stria vascularis; SV, scala vestibuli. The box is enlarged in **b, c**. Barttin (green) and KCNQ1 (red) in adult stria vascularis. **d**, PO cochlea co-stained for barttin (green) and CIC-K (red) reveals complete colocalization (yellow). **e**, Dark cells surrounding the crista ampullaris (CA) express barttin (green) and KCNQ1 (red). Scale bar in **a** indicates 38 μm in **a**, 7 μm in **b**, 22 μm in **c** and **d**, and 31 μm in **e**.

which identifies α -intercalated cells²⁰, both acid-secreting α -intercalated cells and base-secreting β -intercalated cells express barttin basolaterally (Fig. 4k), but intervening aquaporin-2-expressing (green) principal cells²¹ appear devoid of barttin (Fig. 4l).

In the inner ear, barttin colocalized with CIC-K in K^+ -secreting marginal cells of the stria vascularis (Fig. 5d). The basolateral staining for both proteins contrasts with the apical localization of the KCNQ1 K^+ channel (Fig. 5a–c). Previous work²² has identified CIC-K-like currents in marginal cells and correlated them with the presence of CIC-K1 messenger RNA. Our experiments with polymerase chain reaction after reverse transcription (RT-PCR) revealed that not only CIC-K1, but also CIC-K2, was expressed in the cochlea (see Supplementary Information C), indicating that both isoforms are expressed in stria vascularis. Barttin (green, Fig. 5e) was also found in K^+ -secreting vestibular dark cells, where it colocalized in basolateral membranes with CIC-K (not shown) below apical membranes that expressed KCNQ1. No balance problems were reported in BSND, but humans can adapt well to vestibular disturbances²³.

This work has identified a β -subunit for CIC-K Cl^- channels. In the kidney, CIC-K/barttin heteromers mediate Cl^- reabsorption by facilitating its basolateral efflux (Fig. 6a). In the stria, CIC-K/barttin channels drive K^+ secretion by recycling Cl^- for the basolateral NKCC1 cotransporter (Fig. 6b). This role is analogous to that of ROMK in Cl^- -reabsorbing cells of the thick ascending limb, where it recycles K^+ for the apical NKCC2 cotransporter (Fig. 6a).

Because barttin is crucial for CIC-Kb function, its inactivation results in renal salt wasting as do mutations in CIC-Kb³. However, because barttin also associates with CIC-Ka, additional symptoms are expected. These may resemble the diabetes insipidus-like phenotype observed on disrupting mouse CIC-K1 (ref. 10). Indeed, BSND patients present with more severe renal symptoms than patients having mutations in CIC-Kb^{4,24}. Unlike mutations in barttin⁴, mutations in the CIC-Kb α -subunit³ do not cause deafness, nor was deafness described in mice disrupted for CIC-K1 (ref. 10).

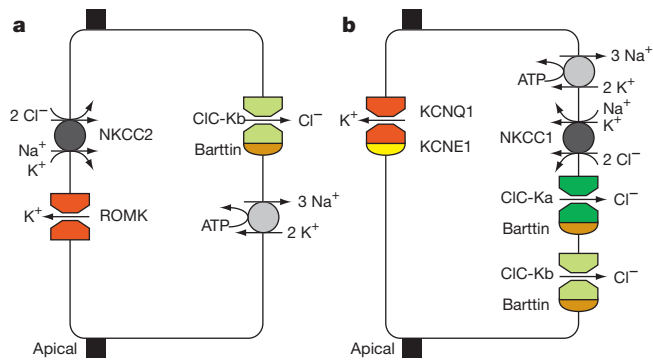


Figure 6 Model for renal Cl⁻ reabsorption (a), and for K⁺ secretion in the stria vascularis (b). **a**, In cells of the renal thick ascending limb, apical NKCC2 cotransporters driving Cl⁻ uptake require ROMK to recycle K⁺. Cl⁻ exits through channels containing CIC-Kb α -subunits and barttin β -subunits. Mutations in all four genes cause Bartter's syndrome¹⁻⁴. **b**, In strial marginal cells, basolateral NKCC1 raises intracellular K⁺ concentration. Parallel CIC-Ka/barttin and CIC-Kb/barttin channels recycle Cl⁻. K⁺ exits through channels containing KCNQ1 α -subunits and KCNE1 β -subunits. Loss of KCNQ1 (ref. 27), KCNE1 (ref. 28), NKCC1 (refs 25, 26) or barttin⁴ causes deafness. Neither loss of CIC-K1 (the orthologue of CIC-Ka)¹⁰ nor of CIC-Kb³ alone entails deafness.

We propose that both CIC-K1 and CIC-K2 are present in basolateral membranes of K⁺-secreting marginal cells (Fig. 6b). Whereas a loss of one of these α -subunits should reduce basolateral recycling of Cl⁻ somewhat, the mutational inactivation of the common β -subunit may abolish recycling completely. As with a disruption of the NKCC1 cotransporter^{25,26}, or with mutations in either subunit of the apical KCNQ1/KCNE1 K⁺ channel^{27,28}, the resulting impairment of K⁺ secretion and endolymph production probably explains the congenital deafness observed in BSND. □

Methods

Functional expression in *Xenopus* oocytes

Capped complementary RNA of CLC channels (10 ng) and barttin (5 ng) were expressed in *Xenopus* oocytes as described¹². Mutations were introduced by recombinant PCR and sequenced. Measurements were in ND96 medium (96 mM sodium chloride, 2 mM potassium chloride, 1.8 mM calcium chloride, 1 mM magnesium chloride and 5 mM HEPES buffer at pH 7.4). For anion replacement, 80 mM Cl⁻ was substituted by equivalent amounts of Br⁻, I⁻ or NO₃⁻. At pH 5.4 or 6.4, HEPES was replaced by 5 mM MES buffer, and at pH 8.4 by 5 mM Tris buffer.

Patch-clamp experiments of transfected cells

tsA201 cells were transiently transfected with complementary DNAs inserted into pCIneo vector with Lipofectamin (Invitrogen). Currents were measured after 2–3 days in the whole-cell mode of the patch-clamp technique using 3–5-M Ω pipettes and an Axopatch 200-A amplifier. The bath solution contained 130 mM sodium chloride, 5 mM potassium chloride, 2 mM magnesium chloride, 2 mM calcium chloride and 10 mM HEPES at pH 7.4. For ion selectivity measurements, Cl⁻ was exchanged for Br⁻ or I⁻. Pipette solutions contained 130 mM caesium chloride, 5 mM sodium chloride, 2 mM calcium chloride, 2 mM magnesium chloride, 10 mM HEPES and 5 mM EGTA at pH 7.4.

Measurement of surface expression

Haemagglutinin (HA) epitopes were introduced between transmembrane domains D8 and D9 of CIC-Ka, CIC-Kb and CIC-1. This did not interfere with their ability to generate currents. Surface expression used HA antibodies and chemiluminescence was as described^{13,14}.

Antibodies

The generation of rabbit and guinea-pig antisera against barttin is described in Supplementary Information D. Published antibodies against CIC-K⁷, KCNQ1 (ref. 29), AE1 (ref. 20) and aquaporin-2 (ref. 21), and commercial antibodies against ROMK (Chemicon), Tamm-Horsfall protein (Dunn), myc epitope (9E10; American Type Culture Collection, ATCC) and HA epitope (3F10; Roche) were used. Fluorophore-coupled secondary antibodies were from Molecular Probes and Jackson.

Immunohistochemistry

Anaesthetized adult mice were perfused through the left ventricle with PBS followed by 4% paraformaldehyde (PFA) in PBS. Adult cochlea were decalcified with Rapid Bone Decalcifier (Eurobio). Inner ears from newborn mice were fixed after dissection. Tissue samples were mounted in OCT compound (Tissue Tek) for cryosections or embedded in paraffin and cut

to 8–12- μ m sections. Sections were fixed in 4% PFA, 0.1% desoxycholate and 0.2% NP40 in PBS, washed, and blocked in 2% BSA, 3% goat serum and 0.5% NP40 in PBS. Antisera were applied in 2% BSA and 0.5% NP40 in PBS. Analysis was by confocal microscopy (Leica).

Received 4 October; accepted 26 October 2001.

- Simon, D. B. *et al.* Bartter's syndrome, hypokalaemic alkalosis with hypercalciuria, is caused by mutations in the Na-K-2Cl cotransporter NKCC2. *Nature Genet.* **13**, 183–188 (1996).
- Simon, D. B. *et al.* Genetic heterogeneity of Bartter's syndrome revealed by mutations in the K⁺ channel, ROMK. *Nature Genet.* **14**, 152–156 (1996).
- Simon, D. B. *et al.* Mutations in the chloride channel gene, *CLCNKB*, cause Bartter's syndrome type III. *Nature Genet.* **17**, 171–178 (1997).
- Birkenhäger, R. *et al.* Mutations of *BSND* causes Bartter syndrome with sensorineural deafness and kidney failure. *Nature Genet.* **29**, 310–314 (2001).
- Jentsch, T. J. Neuronal KCNQ channel: physiology and role in disease. *Nature Rev. Neurosci.* **1**, 21–30 (2000).
- Kieferle, S., Fong, P., Bens, M., Vandewalle, A. & Jentsch, T. J. Two highly homologous members of the CIC chloride channel family in both rat and human kidney. *Proc. Natl Acad. Sci. USA* **91**, 6943–6947 (1994).
- Vandewalle, A. *et al.* Localization and induction by dehydration of CIC-K chloride channels in the rat kidney. *Am. J. Physiol.* **272**, F678–F688 (1997).
- Kobayashi, K., Uchida, S., Mizutani, S., Sasaki, S. & Marumo, F. Intrarenal and cellular localization of CIC-K2 protein in the mouse kidney. *J. Am. Soc. Nephrol.* **12**, 1327–1334 (2001).
- Uchida, S. *et al.* Localization and functional characterization of rat kidney-specific chloride channel, CIC-K1. *J. Clin. Invest.* **95**, 104–113 (1995).
- Matsumura, Y. *et al.* Overt nephrogenic diabetes insipidus in mice lacking the CLC-K1 chloride channel. *Nature Genet.* **21**, 95–98 (1999).
- Uchida, S. *et al.* Molecular cloning of a chloride channel that is regulated by dehydration and expressed predominantly in kidney medulla. *J. Biol. Chem.* **268**, 3821–3824 (1993); erratum *J. Biol. Chem.* **269**, 19192 (1994).
- Waldegger, S. & Jentsch, T. J. Functional and structural analysis of CIC-K chloride channels involved in renal disease. *J. Biol. Chem.* **275**, 24527–24533 (2000).
- Zerangue, N., Schwappach, B., Jan, Y. N. & Jan, L. Y. A new ER trafficking signal regulates the subunit stoichiometry of plasma membrane K_{ATP} channels. *Neuron* **22**, 537–548 (1999).
- Schwake, M., Friedrich, T. & Jentsch, T. J. An internalization signal in CIC-5, an endosomal Cl⁻ channel mutated in Dent's disease. *J. Biol. Chem.* **276**, 12049–12054 (2001).
- Jentsch, T. J., Friedrich, T., Schriever, A. & Yamada, H. The CLC chloride channel family. *Pflügers Arch. Eur. J. Physiol.* **437**, 783–795 (1999).
- Staub, O. *et al.* WW domains of Nedd4 bind to the proline-rich PY motifs in the epithelial Na⁺ channel deleted in Liddle's syndrome. *EMBO J.* **15**, 2371–2380 (1996).
- Schild, L. *et al.* Identification of a PY motif in the epithelial Na channel subunits as a target sequence for mutations causing channel activation found in Liddle syndrome. *EMBO J.* **15**, 2381–2387 (1996).
- Staub, O. *et al.* Regulation of stability and function of the epithelial Na⁺ channel (ENaC) by ubiquitination. *EMBO J.* **16**, 6325–6336 (1997).
- Konrad, M. *et al.* Mutations in the chloride channel gene *CLCNKB* as a cause of classic Bartter syndrome. *J. Am. Soc. Nephrol.* **11**, 1449–1459 (2000).
- Alper, S. L., Natale, J., Lodish, H. F. & Brown, D. Subtypes of intercalated cells in rat kidney collecting duct defined by antibodies against erythroid band 3 and renal vacuolar H⁺-ATPase. *Proc. Natl Acad. Sci. USA* **86**, 5429–5433 (1989).
- Nielsen, S., DiGiovanni, S. R., Christensen, E. L., Knepper, M. A. & Harris, H. W. Cellular and subcellular immunolocalization of vasopressin-regulated water channel in rat kidney. *Proc. Natl Acad. Sci. USA* **90**, 11663–11667 (1993).
- Ando, M. & Takeuchi, S. mRNA encoding 'CIC-K1, a kidney Cl⁻ channel' is expressed in marginal cells of the stria vascularis of rat cochlea: its possible contribution to Cl⁻ currents. *Neurosci. Lett.* **284**, 171–174 (2000).
- Baloh, R. W. Vertigo. *Lancet* **352**, 1841–1846 (1998).
- Jeck, N. *et al.* Hypokalaemic salt-losing tubulopathy with chronic renal failure and sensorineural deafness. *Pediatrics* **108**, E5 (2001).
- Delpire, E., Lu, J., England, R., Dull, C. & Thorne, T. Deafness and imbalance associated with inactivation of the secretory Na-K-2Cl co-transporter. *Nature Genet.* **22**, 192–195 (1999).
- Dixon, M. J. *et al.* Mutation of the Na-K-Cl co-transporter gene *Slc12a2* results in deafness in mice. *Hum. Mol. Genet.* **8**, 1579–1584 (1999).
- Neyroud, N. *et al.* A novel mutation in the potassium channel gene *KVLQT1* causes the Jervell and Lange-Nielsen cardioauditory syndrome. *Nature Genet.* **15**, 186–189 (1997).
- Schulze-Bahr, E. *et al.* *KCNE1* mutations cause Jervell and Lange-Nielsen syndrome. *Nature Genet.* **17**, 267–268 (1997).
- Dedek, K. & Waldegger, S. Colocalization of KCNQ1/KCNE channel subunits in the mouse gastrointestinal tract. *Pflügers Arch. Eur. J. Physiol.* **442**, 896–902 (2001).

Supplementary Information accompanies the paper on Nature's website (<http://www.nature.com>).

Acknowledgements

We thank S. Alper for the AE1 antibody, M. Knepper for the aquaporin-2 antibody, M. Knipper for advice on inner ear immunohistochemistry, and J. Enderich and M. Kolster for technical assistance. R.E. is a recipient of a Marie Curie Human Potential Fellowship of the European Union, and F.H. is a Heisenberg scholar of the Deutsche Forschungsgemeinschaft (DFG). This work was supported by grants from the DFG, the Fonds der Chemischen Industrie, and the Prix Louis Jeantet de Médecine to T.J.J., and from the Federal State of Baden-Württemberg to F.H.

Competing interests statement

The authors declare that they have no competing financial interests.

Correspondence and requests for materials should be addressed to T.J.J. (e-mail: jentsch@zmn.uni-hamburg.de).